Mechanism of Electrochemical Al Deposition from Room-Temperature Chloroaluminate Ionic Liquids

Sang Jung Ahn,† Kwanghoon Jeong, and Jae-Joon Lee*

*Department of Applied Chemistry & Department of Advanced Technology Fusion, Konkuk University, Chungju 380-701, Korea. *E-mail: jjlee@kku.ac.kr*
†Korea Research Institute of Standard and Science, Yuseong, Daejeon 305-340, Korea
Received August 4, 2008, Accepted October 6, 2008

Key Words: Molten salt, Ionic liquid, Aluminum, Electrochemical deposition

Electrochemical deposition of aluminum is of interest because of its potential application in secondary batteries[1,2] and its alloy formation with other transition metals to take advantage of the unique properties of Al. In particular, aluminum based alloy materials such as the light weight transition metal-aluminum alloys have long been an interest because of their structural properties with high strength, environmental stability, and corrosion resistance at elevated temperature. We have studied previously the deposition of aluminum and the formation/growth of Au-Al intermetallic compounds directly on polycrystalline gold electrode, Au(poly),[3] and by using electrochemical quartz crystal microbalance (EQCM)[4] with a special emphasis on the underpotential deposition of Al on Au. Also, the characteristics of the initial stage of the electrochemical aluminum deposition has been continuously studied on various substrates including a carbon-based nonmetal electrodes such as glassy carbon, a boron-doped diamond (BDD), and a nitrogen-incorporated tetrahedral amorphous carbon (taC:N), a conducting diamond-like carbon.[5,6] For these systematic studies, an acidic composition of the $AlCl_3$/1-ethyl-3-methyl imidazolium chloride (EMIC), a chloroaluminate room-temperature ionic liquid, was used as the electrolyte for a quantitative electrochemical aluminum deposition. One of the most interesting features of this melts is the adjustable Lewis acidity and the ionic composition dependent on the $AlCl_3$/EMIC molar ratio, N. Melts with N > 1, or N < 1, are known to be Lewis acidic or Lewis basic, respectively, while those with N = 1 are referred to as neutral. Further information and characteristics of this useful ionic liquids were very well summarized elsewhere at length.[7,8] Figure 1 showed the cyclic voltammograms for the electrochemical deposition and corresponding anodic dissolution of aluminum at Au(poly), W, and GC electrodes in acidic $AlCl_3$/EMIC (N = 1.5). As clearly indicated in these voltammograms, in general, the electrochemical metal deposition requires the electrochemical nucleation and it is usually preceded by the underpotential deposition (UPD) depends on the properties of electrodes. The UPD waves and corresponding stripping peaks at Au and W electrodes indicate that the interaction between these substrates and aluminum is thermodynamically more favorable than that between the same kinds.

The most intriguing issue is the mechanism of electrochemical deposition of Al from $AlCl_3$/EMIC melts particularly at the electrode that having a strong UPD interaction with Al. The aluminum tetrachloride anion, $AlCl_4^-$, is the major anionic species of this melt without regard to the composition (or acidity) but Al deposition is observed only in acidic condition (N > 1) by reduction of $Al_2Cl_7^-$ *via*[9]

$$4Al_2Cl_7^- + 3e^- \leftrightarrow Al + 7AlCl_4^- \quad (1)$$

Therefore, it is expected that there is a significant difference in the mechanism of electrochemical deposition of Al between from a conventional bath and from this kind of room-temperature ionic liquid system. The ambiguity and uniqueness of this system is arisen also from the fact that both $AlCl_4^-$ and $Al_2Cl_7^-$ can induce the Al deposition in a similar inorganic high temperature ionic liquid systems where binary or ternary mixture of alkali metal chloride was used instead of the organ-

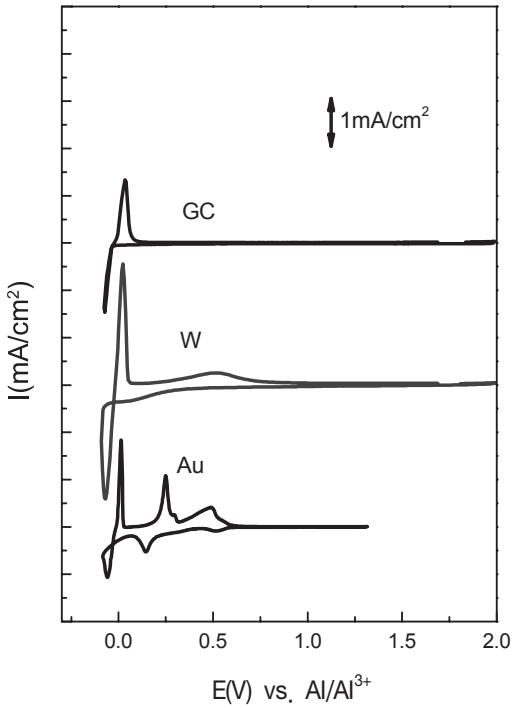

Figure 1. Cyclic voltammetry on Au, W, and GC, in acidic $AlCl_3$/EMIC melts (N = 1.5). The scan rate (v) is 20 mV/s at Au and 100 mV/sec for the other electrodes. The reference electrode was an Al wire immersed in the same solution in which the experiments were performed.

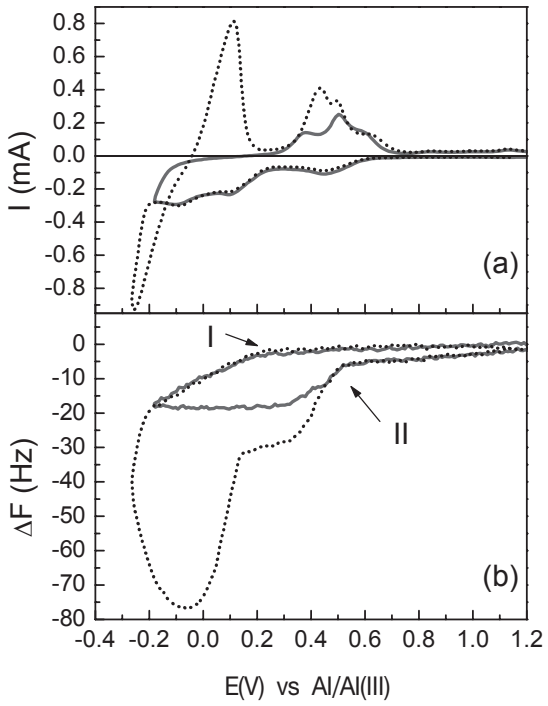

Figure 2. (a) Cyclic voltammetry on Au-QCM showing the differences in anodic dissolution before and after the initiation of the Al bulk deposition in 1/1 v/v acidic (1.1:1) $AlCl_3$/EMIC melt/benzene mixture while the QCM frequency response is monitored. (b) Corresponding *in situ* frequency responses. Al wire immersed in the same solution was used as the reference electrode. Scan rate = 100 mV/s.

ic chloride salts.[10] EQCM study has been performed onto Au (111) films (500 nm in thickness) deposited on a 6 MHz AT-cut, optically polished quartz crystal (2.5 diam) to study the initial stage of the electrochemical deposition of Al from this ionic liquid. In this work, we have used the benzene as a cosolvent to overcome the high viscosity problem of the pure ionic liquid.[4,11] Figure 2 showed the typical voltammetric responses and corresponding frequency shift caused by the mass changes at the EQCM during the electrochemical Al deposition. The solid line represents the case when the bulk deposition of Al was not initiated yet. Generally, the Sauerbrey equation can be applied to a simple deposition process where a linear correlation between the frequency shift (ΔF) and the mass change (Δm, μg/cm^2).[12] Figure 3 showed the plot of ΔF *vs.* Δm during Al deposition. A linear relation, with a slope of ~ 79.0 Hz cm^2/μg, was found in the range between 0.05 and 0.27 μg/cm^2. This is consistent with the theoretically calculated sensitivity factor, 81.4 Hz cm^2/μg, for the quartz crystal used for these measurements. It is notable that initially the resonant frequency decreases slowly by up to ~ 2.6 Hz, for every negative scan, until the potential reaches ~ 0.23V (indicated by I, Figure 2), followed by further decrease up to ~19.8 Hz, with higher rate (dΔF/dE), before the onset of Al bulk deposition with nucleation. The frequency shifts in this range are attributed to the UPD of Al and the formation of surface alloy layers before the onset of bulk Al deposition. Upon switching the scan direction to positive, in case there is no bulk Al deposition, the resonant frequency is maintained till the anodic dissolution of Al is also seen from either UPD or Al/Au alloy layers. However, the resonant frequency increases rapidly along with the dissolution of Al until the potential reaches *ca.* +0.53 V (region II in Figure 2), which is believed to be the potential of the onset of Al dissolution from the UPD layer only. Then, the frequency keeps increasing as the potential scan continues and ultimately returns to its initial value.

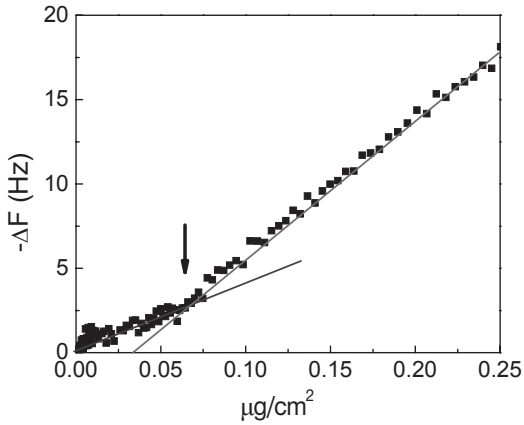

Figure 3. Correlation between the frequency shift (ΔF) and the effective mass change (Δm, μg/cm^2) calculated from the charge obtained by integration of the current response in voltammograms. Solid line represents the calculated frequency shift for given values of mass loaded from Sauerbrey equation. The slope of the best linear fit in the region 0.05 < Δm < 0.27 μg/cm^2, yielded a value of 79.0 Hz cm^2/μg.

An insight into the mechanism of the Al deposition was obtained from the closer inspection of the rate of the frequency change at a smaller mass change region (a mass range between 0.0 and 0.05μg/cm^2). An interesting feature is the slow rate of frequency changes for the first UPD of Al (region I) and the dissolution of a full monolayer of Al UPD after enough Al deposition (region II) in addition to the much smaller slope for the ΔF *vs.* Δm. Both processes are ranging over wide potential region while this feature could not be identified in voltam metric data because it shows the current response only. It implies the possibility that both cathodic and anodic reactions, particularly for Al UPD region, are accompanied by strong interaction between Au and electrolytes at the interface. These can be reasonably explained by considering the existence of an intermediate state consists of partially adsorbed Al^{3+} ion on Au electrode, followed by the fast electrochemical reduction/

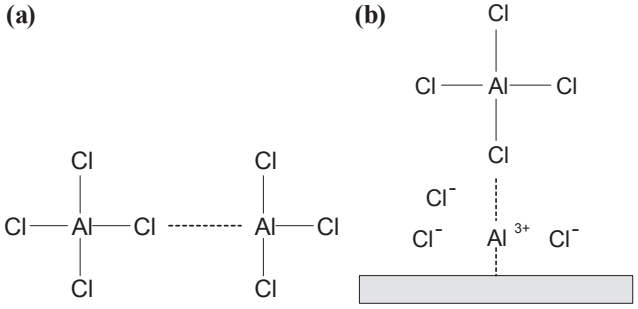

Scheme 1. Visual representation of the intermediate states for Al deposition in $AlCl_3$/EMIC melts. (a) Originally suggested in reference 16. (b) Partially adsorbed Al before and after (region I and II, respectively indicated in Figure 2) electrochemical reaction has occurred.

oxidation of Al, particularly in Al underpotential region as described in Scheme 1. Conventionally, the double layer for the metal-ionic liquid interface is described by a quasi-lattice structure of alternating multilayer of oppositely charged ions under the influence of the electric field, from the earlier studies of electrical double layer in molten salts including mercury electrode in $AlCl_3$/1-butylpiridinum chloride (BPC) melts.[13] It is ordinary to expect that both $Al_2Cl_7^-$ and $AlCl_4^-$, the major anionic components participating in Al deposition and dissolution (Eq. (1)),[14,15] form the closest layer for the electrolyte-side capacitance region in this positive potential range. The anionic composition at the very first layer, throughout the positive potential region, is varying with the potential and the contribution from the larger $Al_2Cl_7^-$ ion, responsible for Al deposition, is keep increasing as the potential is scanned negatively. As a result, the formation of this intermediate state is feasible due to the increasing contribution of $Al_2Cl_7^-$ to the closest capacitive layer at less positive potential (particularly when approaching underpotential region) as well as the strong tendency of UPD interaction between Al and Au. Furthermore, this intermediate state can be stabilized by $AlCl_4^-$, mostly originated from parent $Al_2Cl_4^-$ ion, at the electrolyte side as visualized in Scheme 1. The formation of this intermediate state could be considered as an additional step for the step-wise deposition process suggested by Lai and Skyllas-Kazacos[16] and highly applicable for any substrate even though it is most effectively attributable to substrates, such as Au and W, showing a strong UPD interaction with Al. It is reasonable to consider that the overall process of this intermediate formation is very slow due to the reorganization of the molecular structure of stable $Al_2Cl_7^-$ for proper orientation. It results in the slow down of the overall frequency shift over the wide positive potential range. A similar rationale is also applicable to the dissolution process of a full UPD layer shown in region II. The overall frequency shift at region I, *ca.* 2.6 Hz, less than a full monolayer of Al (5.8 Hz), could be considered as another evidence of the existence of partially adsorbed intermediate state. The relatively lower coverage is mostly attributed to the bulky size and orientation of $Al_2Cl_7^-$ and the overall experimental observations and interpretations are similar to the mass compensation effect reported by Gordon *et al.*[17]

In this note, we have shown the existence of the intermediate species for the electrochemical deposition of alumi num from ionic liquids. This scheme could not be identified from the electrochemical responses only but highly consistent with the interpretation of the EQCM frequency change which represents the mass change at the electrode surface during deposition. However, further studies are required to obtain any optical and spectroscopic evidence for the existence of the intermediate and we are constantly working on this. Nevertheless, it is expected to deduce an important clue from this mechanism to explain the electrochemical deposition of Al in the buffered neutral composition of this kind of ionic liquid system and it is still under investigation.

Experimental Section

A Lewis acidic melt of $AlCl_3$/EMIC with N = 1.5 were prepared and used without further purification for electrochemical Al deposition on various electrodes. A tungsten rod, a glassy carbon (GC) rod, and a polycrystalline gold wire sealed in epoxy, exposing circular surface areas *ca*. 0.08, 0.07 and 0.02 cm^2, respectively, were used as working electrodes. The reference and counter electrode were Al wire and coils (Alfa/AESAR, 99.999%), respectively, immersed in the same meltsin which the experiments were performed unless stated otherwise. For EQCM, a freshly distilled benzene (HPLC, Fisher Scientific), from sodium benzophenone ketyl, was mixed with $AlCl_3$/EMIC (N = 1.1) up to equal volume ratio (1/1 v/v) to minimized the viscosity. A 6 MHz AT-cut, optically polished quartz crystal (2.5 cm diameter) was purchased from Valpey-Fisher Corp. Polycrystalline Au disk electrodes were prepared by sputtering (Materials Research Corporation, SEM-8620) *ca.*500 nm of gold, onto a 10 - 20 nm Ni undercoating layer, followed by hydrogen flame annealing for 1~2 min to seal possible pinholes on the Ausurface and to have a mirror-like finish. The main EQCM cell compartment was assembled in a dry box and then transferred to the open laboratory for measurements. Potential control was achieved with a Pine RDE3 potentiostat coupled with a PARC 175 universal programmer.

Acknowledgments. This work was supported by the faculty research fund of Konkuk University in 2005.

References

1. Fuller, J.; Osteryoung, R. A.; Carlin, R. T. *J. Electrochem. Soc.* **1995**, *142*, 3632.
2. Carlin, R. T.; Long, H. C. D.; Fuller, J.; Trulove, P. C. *J. Electrochem. Soc*. **1994**, *141*, L73.
3. Lee, J.-J.; Bae, I.; Scherson, D. A.; Miller, B.; Wheeler, K. A. *J. Electrochem. Soc.* **2000**, *147*, 562.
4. Lee, J.-J.; Mo, Y.; Scherson, D. A.; Miller, B.; Wheeler, K. A. *J. Electrochem. Soc.* **2001**, *148*, C799.
5. Lee, J.-J.; Miller, B.; Shi, X.; Kalish, R.; Wheeler, K. A. *J. Electrochem. Soc.* **2000**, *147*, 3370.
6. Lee, J.-J.; Miller, B.; Shi, X.; Kalish, R.; Wheeler, K. A. *J. Electrochem. Soc.* **2001**, *148*, C183.
7. (a) Lipsztajn, M.; Osteryoung, R. A. *J. Electrochem. Soc.* **1983**, *130*, 1968. (b) Melton, T. J.; Joyce, J.; Maloy, J. T.; Boon, J. A.; Wilkes, J. S. *J. Electrochem. Soc.* **1990**, *137*, 3865.
8. (a) Nguyen, D. Q.; Oh, J.; Kim, C. S.; Kim, S. W.; Kim, H.; Lee, H.; Kim, H. S. *Bull. Korean Chem. Soc.* **2007**, *28*(12), 2299 (b) Min, K. H.; Yim, T.; Lee, H. Y.; Kim, H. J.; Mun, J.; Kim, S.; Oh, S. M. ; Kim, Y. J. *Bull. Korean Chem. Soc.* **2007**, *28*(9), 1562
9. Carlin, R. T.; Osteryoung, R. A. *J. Electrochem. Soc.* **1989**, *136*, 1409.
10. Jafarian, M.; Mahjani, M. G.; Gobal, F.; Danaee, I. *J. of Appl. Electrochem.* **2006**, *36*, 1169.
11. Moy, R.; Emmenegger, F.-P. *Electrochim. Acta* **1992**, *37*, 1061.
12. Sauerbrey, G. *Z. Physik* **1959**, *155*, 206.
13. Gale, R. G.; Osteryoung, R. A. *Electrochim. Acta* **1980**, *25*, 1527.
14. Melton, T. J.; Joyce, J.; Maloy, J. T.; Boon, J. A.; Wilkes, J. S. *J. Electrochem. Soc.* **1990**, *137*, 3865.
15. Welch, B. J.; Osteryoung, R. A. *J. Electroanal. Chem.* **1981**, *118*, 455.
16. Lai, P. K.; Skyllas-Kazacos, M. *Electrochim. Acta* **1987**, *32*, 1443.
17. Gordon, J. G.; Melroy, O. R.; Toney, M. F. *Electrochim. Acta* **1995**, *40*, 3.